

## Synthesis and Characterization of Dendrimer-Modified Graphene Oxide Nanocarrier for Loading and Releasing Carboplatin

S. Kaveh<sup>a</sup>, E. Tazikheh-Lemeski<sup>a,\*</sup>, E. Moniri<sup>b</sup>, H. Ahmad Panahi<sup>c</sup> and D. Beiknejad<sup>a</sup>

<sup>a</sup>Department of Chemistry, Gorgan Branch, Islamic Azad University, Gorgan, Iran

<sup>b</sup>Department of Chemistry, Varamin (Pishva) Branch, Islamic Azad University, Varamin, Iran

<sup>c</sup>Department of Chemistry, Central Tehran Branch, Islamic Azad University, Tehran, Iran

(Received 20 December 2020, Accepted 7 April 2021)

### ABSTRACT

Carboplatin is a well-known anticancer drug. It, as a targeted medicine, is loaded onto branched graphene oxide nanoparticles (GONPs). In the present study, polymeric coatings with chitosan (CS) bonded of the fifth dendrimer's generation containing the groups of ethylenediamine (EDA) and methyl methacrylate (MMA) function as a responsive polymer. In order to formulate the dendrimer coating, the graphene oxide surface's last carrier, the precursors are polymerized. Chitosan (polymer sensitive to pH) coating is then applied to the branched graphene oxide surface. Further, the drug release is raised. The final product's average size is 42 nm. The FTIR, TGA, XRD, and SEM-EDX are applied to characterize its various adsorption properties. Physical factors of several adsorption processes, including time, pH, and temperature, are examined applying the final adsorbent. The drug release using the adsorbent coated with a polymer sensitive to pH is more than that without. Drug release tests show pH sensitivity behavior in graphene oxide/dendrimer/chitosan (GO/dendrimer/CS) with 98.8% drug release at acidic (pH = 5.6) and 90% at neutral (pH = 7.4) settings, *i.e.*, in the tumorous cell and the blood pH levels, respectively.

**Keywords:** Graphene oxide, Drug delivery, pH-Sensitive polymer, Dendrimer nanoparticles, Carboplatin, Chitosan

### INTRODUCTION

Among the second generations of platinum-containing drugs, carboplatin is investigated as the most significant and widely used one in hospitals for cancer therapy [1]. Through the covalent bond to DNA, leading to the formation of several flaws in the DNA molecule, it compels the cell to undergo apoptotic death way [2]. As a widely applied cancer drug, carboplatin frequently leads to drastic side effects, such as bowel toxicity [3]. Using nanoparticles to carry such drugs has, to some extent, resolved these effects [4]. The use of nanoparticles as drug delivery systems is one of their applications, targeting a zone of interest [5,6]. Nanoparticles play a key role as a carrier for anticancer drugs, decreasing the side effects of the drugs and delivering a proper unit of the drug to the tumor cells [7]. The nanoparticle size, hydrophilicity, surface charge, and

surface area are significant factors affecting the performance of nanomaterials as drug carriers considerably [8]. Polymers have a substantial role in drafting efficient drug delivery systems [9]. Chitosan (CS) is widely used in drug delivery and other pharmaceutical applications due to its biocompatibility, biodegradability, safety, and nontoxicity [10,11]. However, graphene oxide (GO) has drawn attention due to its perfect properties. The nanoscale particle graphene oxide has been applied as an effective nanocarrier in drug delivery [12,13]. The obtained interest of GO nanoparticles as drug carriers is owing to the conductivity and great surface area, providing the potentiality to load a high value of a drug on its surface [14]. Graphene oxide and modified graphene oxide with organic compounds and ligands [15], as well as covalent bonds [16-19], have been applied in drug delivery systems in several methods, loading the drugs onto the graphene sheets *via*  $\pi$ - $\pi$  bonding and electrostatic interactions. Also, the hydrophilicity of graphene oxide is enhanced by its surface modification [20]. In this survey, the adsorption and

\*Corresponding author. E-mail: elham.tazikheh@gorganiau.ac.ir

desorption of carboplatin anticancer drugs are studied using the synthesis of new graphene oxide nanoscale particles and coating by a pH-sensitive polymer. Optimization of variables such as pH, time, and adsorption isotherm at drug loading, adsorbent capacity, and drug release was studied.

## EXPERIMENTAL

### Materials

Carboplatin (chemical formula =  $C_6H_{12}N_2O_4$ pt, FW = 371.25 g mol<sup>-1</sup>,  $\lambda_{max}$  = 229 nm) made in Iran was purchased from the University of Tehran (Tehran, Iran). Sigma-Aldrich Company prepared graphene oxide (GO), chitosan (CS), and *para* toluene sulfonic acid. Ethanol, amino acid glycine, methyl methacrylate (MMA), ethylenediamine (EDA), methanol, *para* amino phenol, water, and mineral acids were supplied from Merck (Darmstadt, Germany). Buffer composition was used in the range of pH = 3 to 9.

### Instruments

FTIR spectroscopy (FT-IR 400-4000 cm<sup>-1</sup>, AVATAR., Thermo, USA), Field-Emission Scanning Electron Microscope (FESEM) images (MIRA III, TESCAN company, Czech Republic), X energy scattering EDAX spectroscopy MIRA III (TESCAN, Czech Republic), Thermogravimetric analysis (TGA) conducted by TGAQ600 (TA, USA), X-ray diffraction by XRDpw1410 (Philips, Netherlands), and drug release was measured using UV-Vis spectrophotometer (Perkin-lambda 25 (USA)).

### Preparation of Graphene Oxide/Amino Acid

In this research, modified-graphene oxide nanoscale particles were synthesized as follows: Amino acid glycine (1 g) was added to the mixture of graphene oxide (2.5 g) and *para* toluene sulfonic acid (2.5 g, as a catalyst). Ethanol (100 ml) stirring was also performed at room temperature for 48 h by a magnetic stirrer [21]. Finally, to collect the desired sediment, the solution was centrifuged; then, the sediment was dried at room temperature.

### Modification of GO with MMA and EDA (GONPs-MMA/EDA)

In a three-necked flask, 150 ml of methanol solvent, 4 g

of GO/amino acid, and 10-12 ml of MMA were added. The system was refluxed in the nitrogen atmosphere in the oil bath for 24 h at 50 °C to produce the first half generation (GO<sub>G0.5</sub>). After 24 h, the solution was centrifuged; then, the sediment was washed with methanol and dried. In the next step, the dried sediment was reacted by 150 ml of new solvent methanol and 12-15 ml of EDA in a two-necked flask for 24 h at 50 °C in the oil bath; it was refluxed to produce the first generation or half of the second generation (GO<sub>G1</sub>). These two steps were repeated until producing the fifth generation [22]. In the last step, to produce the last half-generation (GO<sub>G5</sub>), it was done by dissolving 0.5 g of *para* amino phenol ligand instead of EDA in 50 ml of methanol, and generation (G<sub>4.5</sub>) entered the system; then, at a temperature of 50 °C in the oil bath and the presence of the air atmosphere, it was refluxed for 24 h. After the reaction, the sediment was centrifuged, washed with methanol, and dried at room temperature.

### Coating GONPs-MMA/EDA with CS

First, 10% chitosan was made in 1% acetic acid solution, final adsorbent (GONPs-MMA/EDA) was added to it, and stirring was performed for 1 h at room temperature. Then, it was centrifuged for 30 min, and the sediment was dried at room temperature.

### Adsorption Experiments

The effective parameters, including pH, temperature, contact time, and the concentration of the initial drug, were checked for examining carboplatin's loading attributes. To this end, in each experiment, three variables were kept constant, and the impact of the fourth variable was tested. For each adsorption experiment, 10 mg of the final product (GO/dendrimer/CS) was used. The adsorption experiments were performed by adding GO/dendrimer/CS to 2-5-10-20-30-30-40-60-80 and 100 mg l<sup>-1</sup>, respectively, of carboplatin drug with the desired pH in 3-9 ranges; solutions were shaken with 250 rpm for 2-5-10-15-30-30-60-60-90-120 and 180 min at 298.15 K temperatures. Finally, carboplatin concentration was measured using UV-Vis spectrophotometer at 229 nm. Then, to investigate the drug-releasing, the final adsorbents (GO/dendrimer and GO/dendrimer/CS) were inserted into the dialyze bag. The whole system was placed once in pH = 7.4 (neutral) and

pH = 5.6 buffer (acidic) at 37 °C for 6 h.

At scheduled distances, samples were taken from the solution, and the carboplatin content of each sample was designated by UV spectroscopy. The dendrimer adsorption capacity was computed using the following equation:

$$q_e = V (C_0 - C_e) / W \quad (1)$$

Where  $C_0$ : the initial concentration,

$C_e$ : the equilibrium concentration ( $\text{mg l}^{-1}$ ),

$V$ : the solution volume (l) and  $W$ : the mass of the used carrier (g).

In this study, to predict the mechanism of adsorption kinetic, pseudo-first-order (PFO) and pseudo-second-order (PSO) are investigated. Here, the linear form of the PFO equation as one of the important experiential models may be described as follows [23,24]:

$$\log(q_e - q_t) = \log q_e - (k_1 t / 2.303) \quad (2)$$

Where  $q_e$  and  $q_t$  are the adsorption capacity at equilibrium and definite times ( $\text{mg g}^{-1}$ ), respectively, and  $k_1$  ( $\text{min}^{-1}$ ) is the constant rate of the PFO kinetic model. Another linear equation of kinetic is PSO, as the well-known model, that can be given as follow [25,26]:

$$t/q_t = (1/k_2 q_e^2) + t/q_e \quad (3)$$

Where  $k_2$  ( $\text{mg g}^{-1} \text{min}^{-1}$ ) is the constant rate of the PSO model. Also, the Intra particle Diffusion (ID) model is applied to more investigate the kinetic adsorption [25]:

$$q_t = k_i t^{0.5} + C_i \quad (4)$$

## RESULTS AND DISCUSSION

### Characterization

**FT-IR spectroscopy.** The manufacture of modified-graphene oxide nanoscale particles of the first generation ( $G_1$ ) and the last generation ( $G_5$ ) with its coating by pH-sensitive polymer was corroborated using FTIR spectra; the results are illustrated in Figs. 1a-d. The FTIR spectra for all of these compounds (GO/amino acid,  $GO_{G1}$ ,  $GO_{G5}$ ,

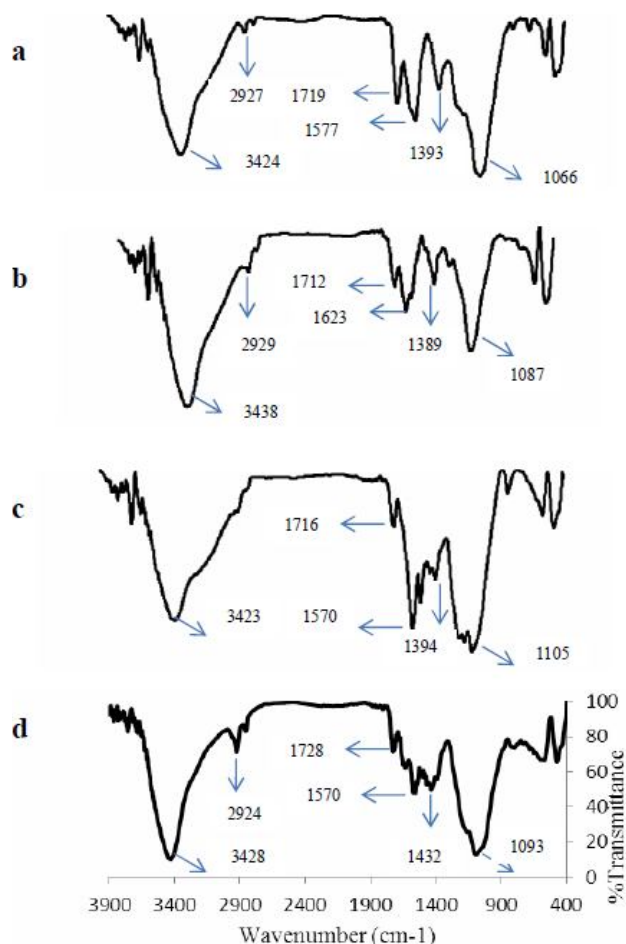


**Fig. 1.** The FTIR spectra of (a) GO/amino acid, (b)  $GO_{G1}$ , (c)  $GO_{G5}$  and (d)  $GO_{G5}/CS$  nanoparticles.

$GO_{G5}/CS$ ) showed specific peaks of about  $3400 \text{ cm}^{-1}$  attributed to stretching vibrations of  $-OH$  and the amine stretch;  $2900$  belonged to asymmetric stretching vibrations of  $-CH_{\text{aliphatic}}$ ;  $1700$  attributed to the  $-C=O$  stretching vibration of ester and amide;  $1600$  associated with  $-NH$  bending of  $NH_2$ ;  $1400$  related to  $-CH-OH$ ;  $1070-1100$  attributed to  $-CO$  [27].

**Field-emission scanning electron microscope (FE-SEM) analysis.** Figures 2a-f shows the illustrations recorded in the contexture and morphology of the first and fifth generations of dendrimer-modified graphene oxide with and without coated chitosan. Figures 2a, b, c, d, e, and

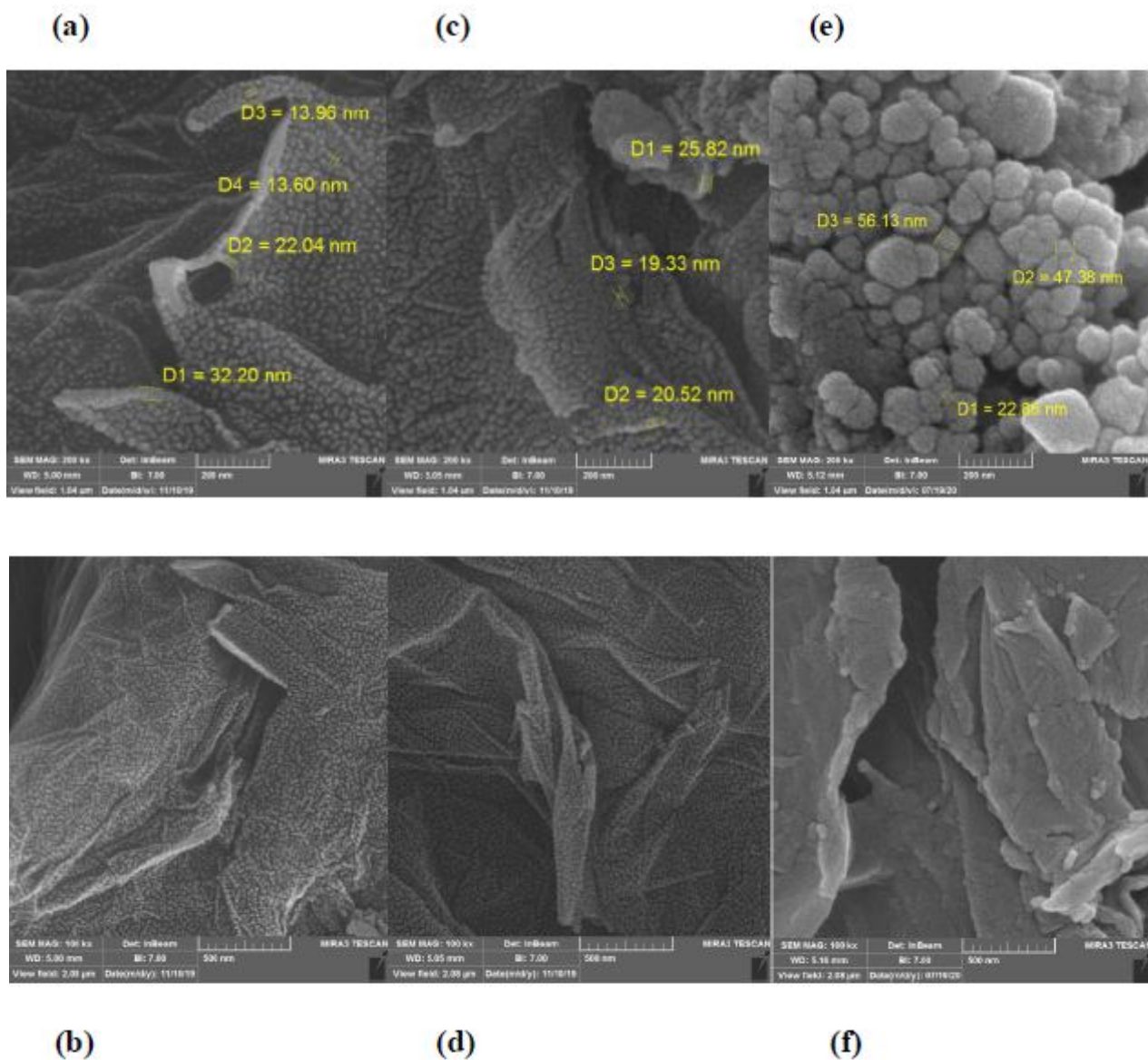


**Fig. 2.** The SEM images of (a, b)  $GO_{G1}$ , (c, d)  $GO_{G5}$  and (e, f)  $GO_{G5}/CS$  Nanoparticles.

f show the morphology of  $GO_{G1}$ ,  $GO_{G5}$ , and  $GO_{G5}/CS$ , respectively. According to the figure, the first and fifth generations of branched graphene oxide nanoscale particles are similar to plates and nearly 21 nm. Images in Figs. 2e, f, spherically measured at almost 42 nm, show a chitosan coating on the surface of the dendrimer-modified graphene oxide. Based on the images, the presence of nano and macro cavities can help the adsorption process.

**Energy dispersive X-ray analysis (EDX).** In Table 1, EDX data for C, N, and O values indicate clear evidence for the first ( $G_1$ ) and fifth ( $G_5$ ) generations of  $GO/dendrimer$  and  $GO_{G5}/chitosan$ , demonstrating that the reaction at the surface of  $GO/dendrimer$  has been performed successfully. The decrease in the atomic percentage of carbon content from  $G_1$  to  $G_5$  can result from the inhibition impact of polymer layers coated on the core particles through all

**Table 1.** EDX Data on the Elemental Compositions of the  $GO_{G_1}$ ,  $GO_{G_5}$  and  $GO_{G_5}/CS$

Element	Atom (%) $G_1$	Atom (%) $G_5$	Atom (%) $G_5/CS$
C	60.63	56.50	58.16
N	17.62	21.66	13.68
O	21.75	21.84	28.16

polymerization steps. On the other hand, the atomic percentage of carbon increases for  $GO_{G_5}/CS$ . It is clear that, in the synthesis of nanoparticles from  $G_1$  to  $G_5$ , due to the increase in nitrogenous compounds, the weight percentage of N atoms in  $G_5$  is higher than  $G_1$  generation. Moreover, whenever chitosan (CS) is added to the nanoscale particles, the weight percentage of the O atom has incremented owing to the presence of the OH groups and oxygen atom in CS; further, the weight percentage of the N atom has reduced due to the nanoscale particles coated by CS.

In Fig. 3, red, blue, and green dots indicate carbon,

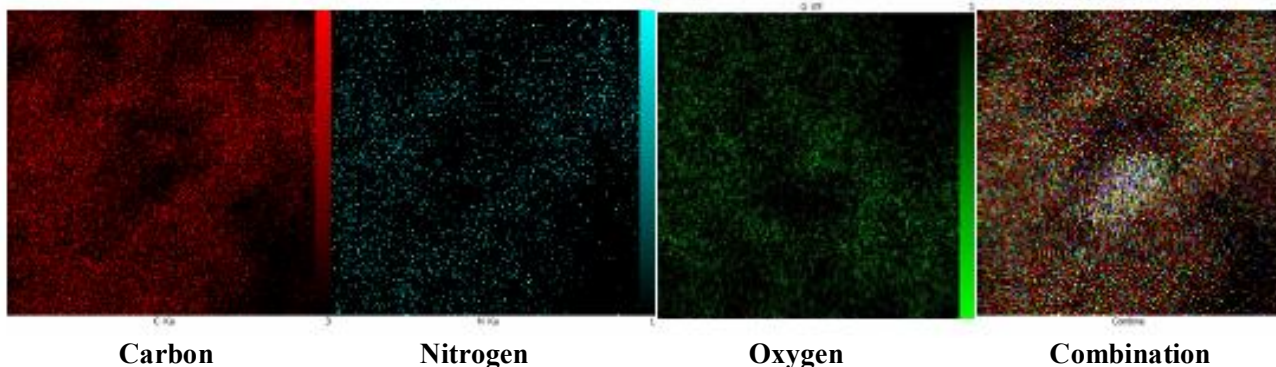


**Fig. 3.** The corresponding EDX maps of C, N, and O elements. (Red: C, Blue: N, Green: O, Combination: C, N and O).

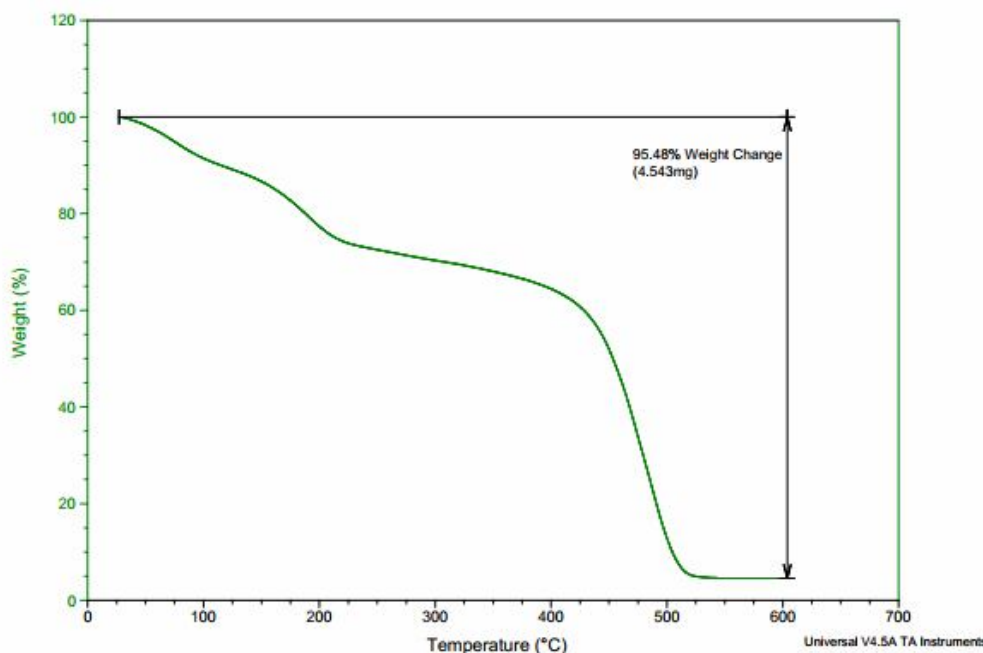


**Fig. 4.** The TGA analysis results of GO/dendrimer nanoparticles.

nitrogen, and oxygen in the nanoparticles, respectively, indicating that the dendrimer is seated on the surface of graphene oxide. The presence of oxygen shows the dendrimer coated by chitosan. Finally, the last image is related to a combined presence of all these elements in the GO/dendrimer nanoparticles.

**Thermo gravimetric (TGA) analysis.** TGA peruses the thermal stability and thermal decomposition of GO<sub>G5</sub> samples (Fig. 4) and compares them to the TGA curve of graphene oxide [28]. As observed in the curve, there are three stages of weight loss. The first occurs at about 100 °C, where the surface water disappears; the second stage happens between 150-250 °C in the weight loss of around 12% observed for G<sub>F</sub>. Finally, at 420 °C, the whole graphene oxide burns to carbon dioxide.

**X-ray diffraction (XRD) analysis.** The crystalline structures of the branched graphene oxide nanoparticles were investigated using the XRD technique. According to the XRD pattern for GONPs-MMA/EDA (Fig. 5a) and its comparison with the XRD pattern of graphene oxide (Fig. 5b) [29], the dendrimers sit on the surface of graphene oxide, and there is no sharp peak of graphene oxide composition.

### Effect of pH

The pH as a significant factor was investigated in the drug adsorption mechanism by nanoparticles. Figure 6 depicts the pH effect on the adsorption of carboplatin on the GO/dendrimer/CS at 293 K. As shown in the figure, by the increment of the pH from 3 to 9, the amount of carboplatin adsorbed by GO/dendrimer/CS increases, possibly due to the various interactions between the adsorbent and carboplatin. The optimal pH for carboplatin adsorption on the surface of the adsorbent was 7. At this pH, carboplatin concentration was the highest value. Moreover, when the pH amount incremented, the GO/dendrimer/CS's surfaces became insignificantly positively charged, increasing electrostatic repulsion force, which would decrease the adsorption of carboplatin onto the adsorbent.

### The Contact Time Effect

The contact time can significantly affect the adsorption percentage of the drug by the nanoparticle. The adsorption efficiency increased with increasing contact time. Figure 7

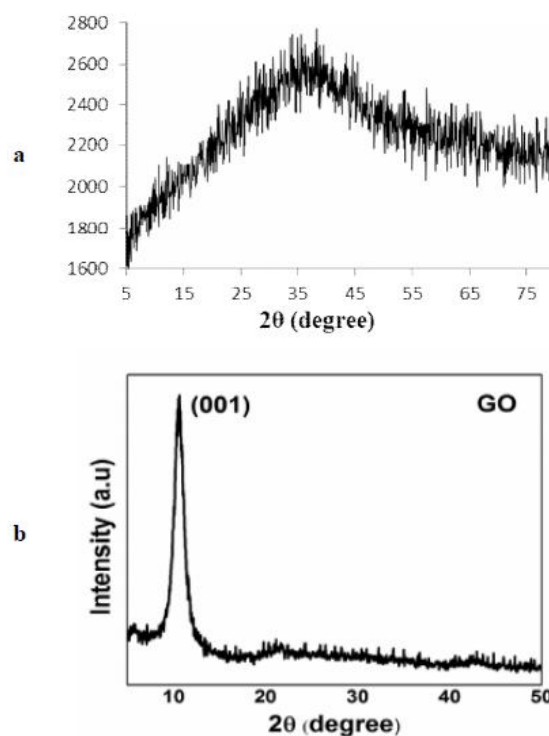


**Fig. 5.** The XRD pattern of (a) GO/dendrimer nanoparticles and (b) GO.

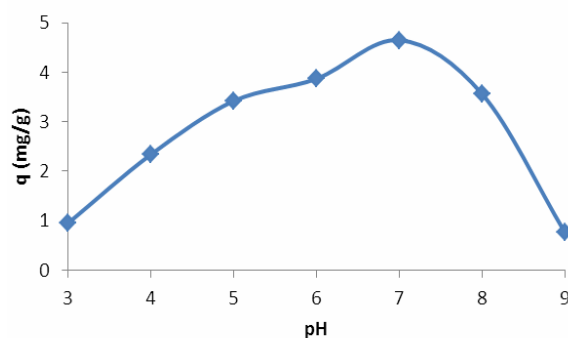


**Fig. 6.** The pH effect in the adsorption of carboplatin onto GO/dendrimer/CS. (Drug concentration = 20 mg l<sup>-1</sup>, Adsorbent dose = 0.01 g).

shows a good adsorption process for carboplatin target in 45 min, with a percentage of 99.9%. The rate of adsorption in 45 min was higher compared to other stages due to the

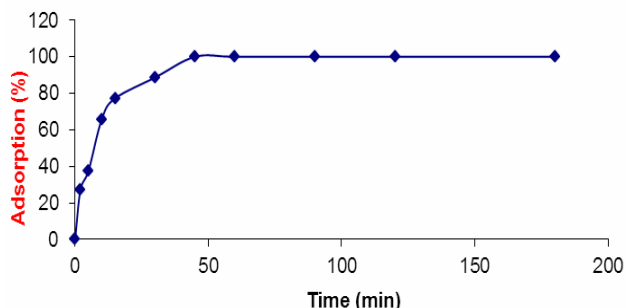


**Fig. 7.** The effect of contact time for the adsorption of carboplatin onto GO/dendrimer/CS. (Drug concentration = 20 mg l<sup>-1</sup>, Adsorbent dose = 0.01 g and pH = 7).

access of more active sites. These data verify the fast kinetics of the process and the carrier's great efficiency in adsorption of the target from the solution. The evenness is reached after 45 min. As the available sites at the surface gradually are filled up, the adsorbed carboplatin molecules tend to be transported to the adsorbents' inner pores. Therefore, the adsorption value remains constant. The kinetic parameters of the models mentioned above are reported in Table 2.

### Adsorption Isotherms

The effect of carboplatin concentration in the range of 2 to 100 mg l<sup>-1</sup> was investigated. Based on the results, the amount of  $q_e$  sharply increases when high doses of the drug are prescribed, while at higher amounts of  $C_e$ , the increased rate of  $q_e$  decreases, indicating that the GO/dendrimer/CS could be entirely saturated at high initial contents of carboplatin drug. Isotherms are also an important factor in the design of adsorption systems, describing the relationship between the concentration and the capacity of an adsorbent. Thus, in this research, Freundlich (F), Langmuir (L), Temkin (T), and Dubinin-Radushkevich adsorption isotherm models were performed at 25 °C. Table 3 presents the calculated isotherm constants by applied models.

As seen in Table 3, the Langmuir model appears more ideally than the other three models ( $R^2 = 0.99$ ) to explain the adsorption process at 25 °C. In this model, the  $q_{max}$  and  $K_L$  coefficients are calculated according to the width of the origin and the slope of the linear graph  $q_e/C_e$ , respectively.

**Table 2.** The Constants of Kinetic Models for Adsorption of Carboplatin onto the GO/Dendrimer/CS

Models	Parameters	Value
Pseudo-first-order	$k_1$ (min <sup>-1</sup> )	0.123
	$q_{e, cal}$ (mg g <sup>-1</sup> )	7.84
	$R^2$	0.985
Pseudo-second-order	$k_2$ (gm g <sup>-1</sup> min <sup>-1</sup> )	0.017
	$q_{e, cal}$ (mg g <sup>-1</sup> )	11.17
	$R^2$	0.998
Intraparticle Diffusion	$K_i$ (mg g <sup>-1</sup> min <sup>-1/2</sup> )	1.48
	$C_i$ (mg g <sup>-1</sup> )	1.42
Experimental data	$R^2$	0.926
	$q_{e, exp}$ (mg g <sup>-1</sup> )	10.73

**Table 3.** The Adsorption of Carboplatin Parameters onto the GO/Dendrimer/CS by Different Isotherms

Isotherm	Parameters	Value
Langmuir	$q_m$ (mg g <sup>-1</sup> )	40
	$K_L$ (l mg <sup>-1</sup> )	0.27
	$R_1$	0.034
	$R^2$	0.99
Freundlich	$K_F$ (mg <sup>1-1/n</sup> l <sup>1/n</sup> g <sup>-1</sup> )	12.82
	$n$	3.60
	$R^2$	0.96
Temkin	$b$ (kJ mol <sup>-1</sup> )	403.69
	$A$ (l mg <sup>-1</sup> )	7.95
	$R^2$	0.98
Dubinin-Radushkevich	$B$	6.14
	$q_s$ (mg g <sup>-1</sup> )	22.02
	$k_{ad}$ (mol <sup>2</sup> kJ <sup>-2</sup> )	$1 \times 10^{-7}$
	$R^2$	0.98

The Langmuir isotherm assumes that the adsorption process occurs at homogeneous sites on the adsorbent; it is used successfully to describe single-layer adsorption. Also, a high  $q_{max}$  value suggests that the adsorption is performed remarkably.

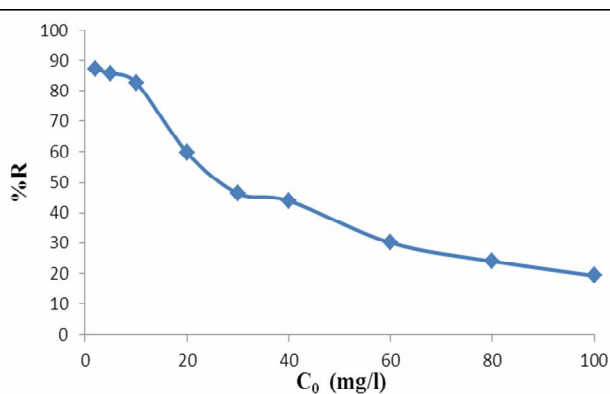


**Fig. 8.** The Percentage of Removal Different concentrations of Carboplatin from GO/dendrimer/CS.

### Adsorption Studies

**Adsorbent optimization.** This experiment was carried out at 25 °C to determine the best adsorption of Carboplatin by GO/dendrimer/CS or the lowest removal percentage (%R) of the drug from the nanocarrier. The effect of carboplatin concentration in the range of 2 to 100 mg l<sup>-1</sup> was investigated. As seen in Fig. 8, the amount of  $q_e$  sharply increases, and the amount of %R decreases when high doses of the drug are prescribed; it means that with an increase of the concentration of the drug ( $C_0$ ), the number of adsorption increases. Amounts of %R are reported in Table 4.

### Drug Release from the G<sub>F</sub> Nanoparticles

It was found that releasing carboplatin by GO/dendrimer and GO/dendrimer/CS at pH = 5.6, similar to the pH of cancer cells, was much more than releasing at pH = 7.4. After one hour, the release of carboplatin from GO/dendrimer was 40.60% at pH = 5.6 and 9.79% at pH = 7.4. Also, the release of carboplatin by GO/dendrimer/CS after one hour was 49.87% at pH = 5.6 and 14.30% at pH = 7.4. Thus, the drug release from the adsorbent coated by chitosan (GO/dendrimer/CS) was more than without CS (GO/dendrimer). After 6 h, the release was almost complete (98.80%) in the presence of CS at pH = 5.6, while it was 93.42% in the absence of CS at pH = 5.6 (Fig. 9). Also, the reaction was equilibrium, and the drug tended to remain on the polymer surface; however, since chitosan is pH-sensitive and shrinks at low pH, drug release was more in the presence of CS (5%).

**Table 4.** The Percentage of Removal Different Concentrations of Carboplatin from GO/Dendrimer/CS

Removal (%)	C <sub>0</sub> (mg l <sup>-1</sup> )	q <sub>e</sub> (mg l <sup>-1</sup> )
87.14	2	3.48
90.76	5	9.07
82.68	10	16.53
59.82	20	23.93
46.45	30	27.87
43.95	40	35.16
30.11	60	36.13
23.97	80	38.36
19.19	100	38.39

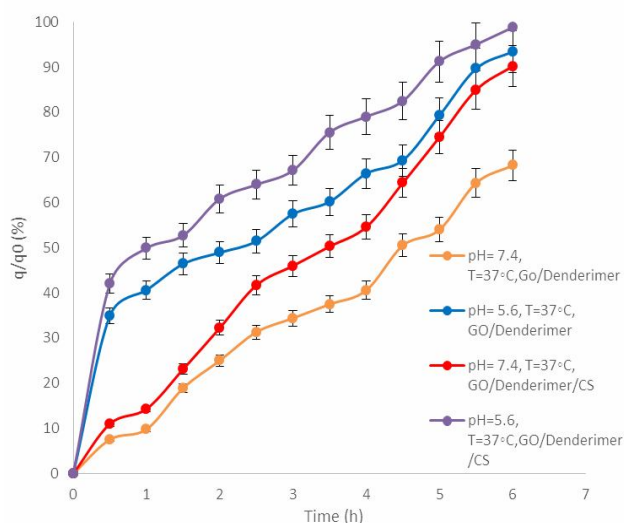


**Fig. 9.** The effect of pH on the release of carboplatin by GO/dendrimer and GO/dendrimer/CS.

## CONCLUSIONS

In this study, the final carrier showed a great response to pH alteration. Graphene oxide nanoparticle was synthesized and used to load carboplatin through the adsorption method in aqueous solution; also, their adsorption capacity for carboplatin solutions was investigated. The optimum pH for loading carboplatin by these nanomaterials was 7, and the



percentage of the drug release in cancer cells at 5.6 was at the highest rate. The most adsorption capacity was observed at the highest concentration of drug and 45 min of contact time. The uppermost sorption capacity,  $q_m$ , could reach 40 mg g<sup>-1</sup> at 298.15 K. Results affirm the modification of graphene oxide surface with dendrimers containing MMA and EDA satisfactorily to produce a drug carrier sorbent product. The comparison of isotherm models indicates the Langmuir model as the best for the equivalence data. The adsorption kinetic fits in the PSO model well ( $R^2 = 0.998$ ) for carboplatin concentrations of 20 (mg l<sup>-1</sup>).

### Funding

Not applicable.

### REFERENCES

- [1] W. Zhang, C. Li, C. Shen, Y. Liu, X. Zhao, Y. Liu, D. Zou, Z. Gao, C. Yue, *Drug Deliv.* 23 (2016) 2575.
- [2] A. Eastman, *Pubmed. Cancer Cells* 2 (1990) 275.
- [3] Y. Chaoheng, Z. Bailing, X. Xuyang, C. Shuang, D. Yun, W. Yantai, W. Lei, T. Yaomei, Z. Binyan, X. Heng, Y. Li, *Cell Death and Disease.* 10 (2019) 714.
- [4] R. Cavalli, M. Argenziano, E. Vigna, P. Giustetto, E. Torres, S. Aime, E. Terreno, *J. Col. Surf. b.* 129 (2015) 39.
- [5] T.M. Allen, P.R. Cullis, *Science* 303 (2004) 1818.
- [6] A.Z. Wilczewska, K. Niemirowicz, K.H. Markiewicz, H. Car, *Pharmacol. Rep.* 64 (2012) 1020.
- [7] R. Singh, J.W. Lillard Jr, *Exp. Mol. Pathol.* 86 (2009) 215.
- [8] D.L. Cooper, C.M. Conder, S. Harirforoosh, *Expert. Opin Drug Deliv.* 11 (2014) 1661.
- [9] P. Agrawal, *J. Pharmacovigil.* 3 (2014) 1.
- [10] M. Dash, F. Chiellini, R.M. Ottenbrite, E. Chiellini, *Prog. Polym. Sci.* 36 (2011) 981.
- [11] J.M. Vaz, D. Pezzoli, P. Chevallier, C.S. Campelo, G. Candiani, D. Mantovani, *Curr. Pharm. Des.* 24 (2018) 866.
- [12] J. Liu, L. Cui, D. Losic, *Acta Biomater.* 9 (2013) 9243.
- [13] Z. Liu, J.T. Robinson, X. Sun, H. Dai, *J. Am. Chem. Soc.* 130 (2008) 10876.
- [14] L. Zhang, J. Xia, Q. Zhao, L. Liu, Z. Zhang, *Nano. Micro Small* 6 (2010) 537.
- [15] K. Vinothini, N.K. Rajendran, A. Ramu, N.K. Elumalai, M. Rajan, *Biomed. Pharmacother.* 110 (2019) 906.
- [16] X. Yang, Y. Wang, X. Huang, Y. Ma, Y. Huang, R. Yang, H. Duan, Y. Chen, *J. Mater. Chem.* 21 (2011) 3448.
- [17] G. Wei, M. Yan, R. Dong, D. Wang, X. Zhou, J. Chen, J. Hao, *Chem. Eur. J.* 18 (2012) 14708.
- [18] X. Sun, Z. Liu, K. Welsher, J.T. Robinson, A. Goodwin, S. Zaric, H. Dai, *Nano Res.* 1 (2008) 203.
- [19] Y. Yang, Y.M. Zhang, Y. Chen, D. Zhao, J.T. Chen, Y. Liu, *Chem. Eur. J.* 18 (2012) 4208.
- [20] M. Namvari, H. Namazi, *Carbohydr. Res.* 396 (2014) 1.
- [21] F. Xiao, M. Guo, J. wang, X. Yan, H. Li, C. Qian, Y. Yu, D. Dai, *Anal. Chim. Acta* 1043 (2018) 35.
- [22] H. Mirzapour, H.A. Panahi, E. Moniri, A. Feizbakhsh, *Micro Chim. Acta* 185 (2018) 9.
- [23] R. Qu, Y. Niu, J. Liu, C. Sun, Y. Zhang, H. Chen, C. Ji, *React. Funct. Polym.* 68 (2008) 1272.
- [24] B.M.W.P.K. Amarasinghe, R.A. Williams, *Chem. Eng. J.* 132 (2007) 299.
- [25] M. Hamayun, T. Mahmood, A. Naeem, M. Muska, S.U. Din, M. Waseem, *Chemosphere* 99 (2014) 207.
- [26] I. Langmuir, *J. Am. Chem. Soc.* 40 (1918) 1361.
- [27] L. Xu, J. Chen, Y. Wen, H. Li, J. Ma, D. Fu, *Desalin. Water Treat.* 57 (2016) 18.
- [28] R. Aghehrochabokia, Y.A. Chabokib, S.A. Malekniac, V. Irani, *J. Environ. Chem. Eng.* 7 (2019) 103285.
- [29] M. Muniyalakshmi, K. Sethuraman, D. Silambarasan, *Materialstoday: Proceedings* 21 (2020) 408.